

Morphotropic phase boundary and electrical properties in $(1-x)\text{Bi}_{0.5}\text{Na}_{0.5}\text{TiO}_3-x\text{Bi}(\text{Zn}_{0.5}\text{Ti}_{0.5})\text{O}_3$ lead-free piezoceramics

Shan-Tao Zhang,^{1,2} Feng Yan,^{1,a)} and Bin Yang³

¹Department of Applied Physics, The Hong Kong Polytechnic University, Hung Hom, Kowloon, Hong Kong

²Department of Materials Science and Engineering and National Laboratory of Solid State Microstructures, Nanjing University, Nanjing 210093, China

³Department of Physics, Center for Condensed Matter Science and Technology, Harbin Institute of Technology, Harbin 150001, China

(Received 20 February 2010; accepted 23 April 2010; published online 10 June 2010)

$(1-x)\text{Bi}_{0.5}\text{Na}_{0.5}\text{TiO}_3-x\text{Bi}(\text{Zn}_{0.5}\text{Ti}_{0.5})\text{O}_3$ [(1-x)BNT-xBZT, $x=0, 0.025, 0.0375, 0.050,$ and 0.075] lead-free piezoceramics were prepared and their structures and electrical properties were investigated. It is found that BZT can increase the Curie temperature of BNT. A morphotropic phase boundary (MPB) separating rhombohedral and tetragonal phases exists near $x=0.0375$. As the result, the MPB composition shows improved electrical properties; the saturated polarization, remnant polarization, and coercive field are $42.0 \mu\text{C}/\text{cm}^2$, $36.5 \mu\text{C}/\text{cm}^2$, and $3.5 \text{ kV}/\text{mm}$, respectively, while the piezoelectric coefficient, planar electromechanical coupling factor, and unipolar strain are $92 \text{ pC}/\text{N}$, 0.22 , and 0.08% , respectively. The structures and electrical properties are discussed by comparing with that of other BNT-based piezoceramics. Our results do not only supplement for BNT-based lead-free piezoceramics, but also may provide a way to develop new lead-free piezoceramics with high Curie temperature. © 2010 American Institute of Physics. [doi:10.1063/1.3431387]

I. INTRODUCTION

Lead-based piezoelectric ceramics exemplified by $\text{Pb}(\text{Zr},\text{Ti})\text{O}_3$ (PZT) are today still essential for commercial electronic devices, e.g., sensors and actuators. However, lead is toxic and consequently should be expelled from device materials, with respect to legislation, as summarized in Ref. 1. Accordingly, many efforts have been devoted to searching for lead-free piezoelectric materials to replace PZT. Some perovskite-based lead-free piezoceramics, mainly based on rhombohedral $\text{Bi}_{0.5}\text{Na}_{0.5}\text{TiO}_3$ (BNT), tetragonal BaTiO_3 (BT), and orthorhombic $\text{K}_{0.5}\text{Na}_{0.5}\text{NbO}_3$ (KNN), have been proposed as promising candidates for replacing PZT.²⁻⁹ BNT has some advantages such as large ferroelectric polarization, high Curie temperature, thus, many BNT-based lead-free piezoceramics have been developed.^{2,6-9} Generally, by introducing other perovskite oxides such as BT and KNN into BNT to form solid solutions, especially when the solid solutions locate in the region of so-called morphotropic phase boundary (MPB) where two different phases coexist, BNT-based piezoceramics can have greatly improved electrical performance.⁶⁻⁸

On the other hand, tetragonal $\text{Bi}(\text{Zn}_{0.5}\text{Ti}_{0.5})\text{O}_3$ (BZT) has been reported to have very high c/a ratio of 1.21 and large calculated ferroelectric polarization of $150 \mu\text{C}/\text{cm}^2$, whereas it is not stable in its pure form and can only be stabilized at high pressure.¹⁰ However, it is reported that BZT-containing solid solutions can be stable in atmospheric condition and still have enhanced c/a ratio, ferroelectric polarization, and increased T_c .¹¹⁻¹⁴ At present, reports on BZT-containing piezoceramics are mainly focused on the solid

solution of tetragonal BZT with other lead-containing tetragonal perovskites such as PbTiO_3 .¹¹⁻¹⁴ Therefore, investigations on its solid solutions with other lead-free counterparts are desirable.

Based on the above motivations, it is interesting to prepare solid solutions of lead-free rhombohedral BNT and tetragonal BZT and investigate their structures and electrical properties. It is expected that BZT may not only improve the T_c of BNT, but also its solid solutions with BNT can form a MPB separating rhombohedral and tetragonal phases, the corresponding MPB composition may have improved electrical properties. In this article, we designed, prepared, and investigated the compositions of $(1-x)\text{BNT}-x\text{BZT}$ with $x=0, 0.025, 0.0375, 0.05,$ and 0.075 .

II. EXPERIMENTAL PROCEDURE

The $(1-x)\text{BNT}-x\text{BZT}$ ($x=0, 0.025, 0.0375, 0.05,$ and 0.075) piezoceramics were prepared by solid state reaction method. Bi_2O_3 (99.8%), Na_2CO_3 (99.8%), TiO_2 (99.0%), and ZnO (99.9%) were chosen as starting raw materials. For each composition, the dried oxides and carbonates were weighed according to the stoichiometric formula $(1-x)\text{BNT}-x\text{BZT}$ with $x=0, 0.025, 0.0375, 0.05,$ and 0.075 and ball milled for 24 h in ethanol. The dried slurries were calcined at 900°C for 3 h and then ball milled again for 24 h. The powders were subsequently pressed into green disks with a diameter of 10 mm under 60 MPa. Sintering was carried out at 1100°C in covered alumina crucibles. To reduce the volatility during firing of Bi, Na, and K, the disks were embedded in the corresponding powder. The crystal structures of the ceramics were characterized by powder x-ray diffraction (XRD) (Rigaku Ultima III) using crushed,

^{a)}Electronic mail: apafyan@polyu.edu.hk.

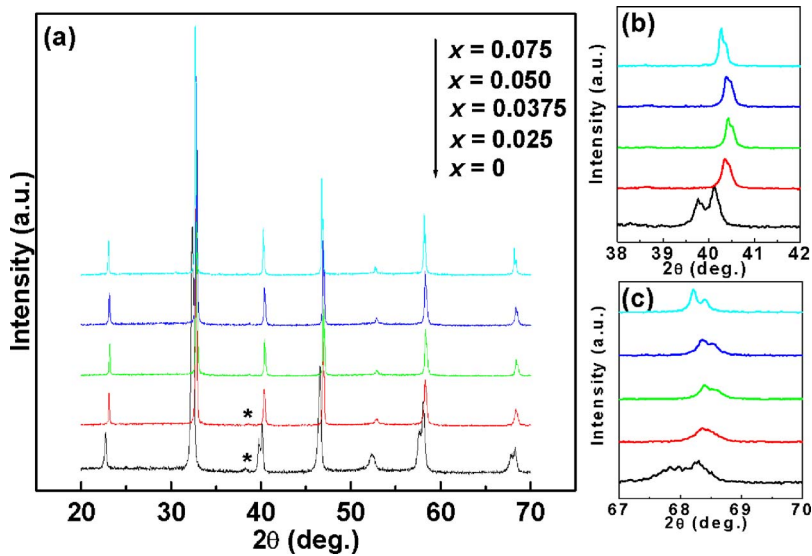


FIG. 1. (Color online) (a) XRD patterns of the piezoceramics, the asterisks indicate the superstructure peak corresponding to the space group of $R3C$, (b) and (c) detailed composition dependent XRD patterns.

unpoled sintered samples. The microstructures were analyzed by using a scanning electron microscopy (SEM, XL30 Philips).

Electric measurements were carried out on sintered ground disks. The circular surfaces of the disks were covered with a thin layer of silver paste and fired at 550 °C for 30 min. Relative dielectric constant (ϵ_r) and loss tangent ($\tan \delta$) of unpoled ceramics were measured using an impedance analyzer (HP4294A) at different frequencies from 100 Hz to 1 MHz in a temperature range from 50–400 °C. Electric measurements were carried out at room temperature in silicone oil. Both polarization-electric field (P-E) and strain-electric field (S-E) curves were measured at 1 Hz by Precision premier II (Radiant Tech. USA). The piezoelectric coefficient (d_{33}) was measured with a Berlincourt- d_{33} -meter (Institute of acoustic, Chinese academic society, ZJ-6A, China). With HP4294A impedance analyzer, the first resonance and anti-resonance frequencies of poled ceramics (poling field 6 kV/mm) were measured and the planar electromechanical coupling factor (k_p) were evaluated on the basis of IEEE standards.

III. RESULTS AND DISCUSSION

Figure 1(a) plots the XRD patterns of the piezoceramics. All ceramics are crystallized into a pure perovskite phase. Interestingly, with increasing x value, some diffraction peaks located at higher angle tend to merge first and then split subsequently. For example, (003) and (021) peaks near $2\theta = 40^\circ$ of pure BNT [Fig. 1(b)] and (024) and (220) peaks near $2\theta = 68^\circ$ of pure BNT [Fig. 1(c)] combine when $x = 0.025$ – 0.0375 and then split with further increasing x . Furthermore, the asterisk in Fig. 1(a) indicates a superstructure peak, which characterizes the space group of $R3C$.¹⁵ This superstructure peak disappears when x reaches 0.0375. In addition, our preliminary Rietveld refinement based on XRD data indicates that, the composition with $x = 0.075$ can be described with tetragonal structure. By considering the above composition dependent XRD patterns and following electrical measurements, a rhombohedral-tetragonal MPB located near $x = 0.0375$ could be identified. It is interesting to note

that the rhombohedral-tetragonal MPB of $(1-x)\text{BNT} - x\text{BZT}$ occurs near $x = 0.0375$ while that the rhombohedral-tetragonal MPB of $(1-x)\text{BNT} - x\text{BT}$ occurs near $x = 0.06$, which is reasonable since the tetragonality of BZT is higher than BT.

All the ceramics have dense and homogeneous microstructures. Typical SEM microstructure image of the composition with $x = 0.0375$ is shown in Fig. 2. It is seen that the ceramics consist of cubicle like grains with the average grain size of ~ 800 nm. No significant composition dependence of grain size can be established.

The relative dielectric constant (ϵ_r) and dielectric loss ($\tan \delta$) are measured as the functions of temperature. The results measured at 10^4 Hz are plotted in Figs. 3(a) and 3(b), respectively. Obviously, the addition of BZT increases the T_c from 290 to 310 °C, consistent with other reports that BZT can lead to increased T_c .^{12–14} However, two important features should be noted in our lead-free piezoceramics, first, the improvement of T_c is about 20 °C, which is not as significant as other BZT-containing systems such as BZT–PbTiO₃.^{12–14} Second, for those compositions with $x > 0.025$, no further increase in T_c can be detected, as can be seen in Fig. 3(a). The above two features may be attributed to that, the content of BZT in our piezoceramics is very low (less than 10%), whereas in other BZT-related systems such as BZT–PbTiO₃, the mole ratio of BZT can reach 40%.¹³ That means, to further understand the effects of BZT on T_c

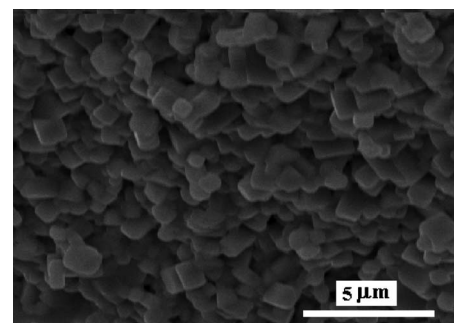


FIG. 2. Typical SEM microstructures of the composition with $x = 0.0375$.

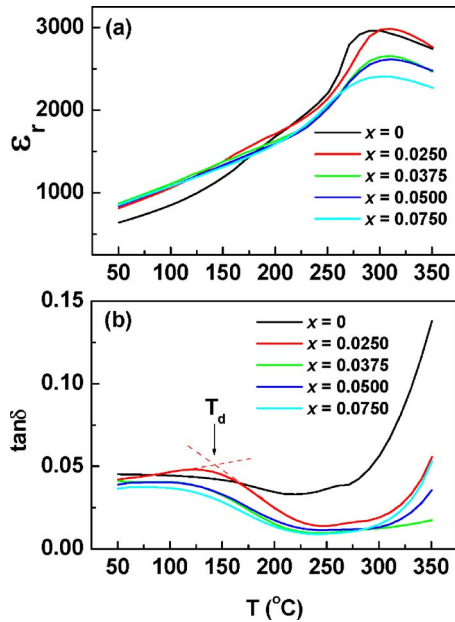


FIG. 3. (Color online) Temperature dependent (a) relative dielectric constant and (b) loss tangent measured at 10^4 Hz.

of BNT, investigations on the ceramics of $(1-x)\text{BNT}-x\text{BZT}$ with higher x value are necessary, this is not the main topic of this work. Additionally, with increasing x , both the ϵ_r value at T_c [Fig. 3(a)] and the depolarization temperature T_d [as indicated by arrow in Fig. 3(b)] tend to decrease, consistent with reports on other BZT- and BNT-related piezoceramics.^{6-9,12-15}

Figure 4 presents the ferroelectric characteristics of $(1-x)\text{BNT}-x\text{BZT}$ ceramics. For the ceramics with $x \leq 0.0375$, well saturated P-E loops can be obtained, typical P-E loop of the composition with $x=0.0375$ is shown in Fig. 4(a). For the compositions with $x=0.050$ and 0.075 , the loops tend to be obviously slimmer. The detailed composition dependence of saturated polarization (P_s), remnant polarization (P_r), and coercive field (E_c) are plotted in Fig. 4(b). As can be seen, the

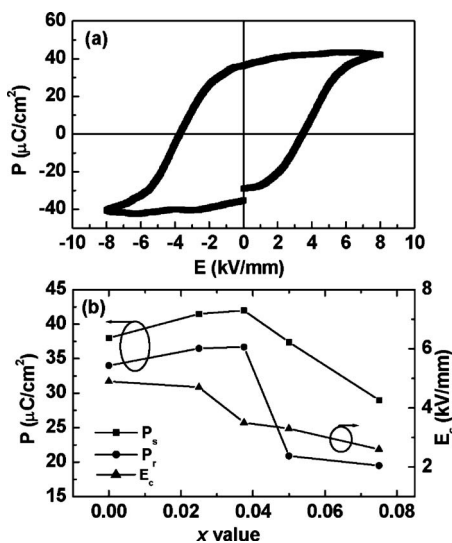


FIG. 4. (a) P-E ferroelectric loops of the composition with $x=0.0375$ and (b) composition dependent P_s , P_r , and E_c .

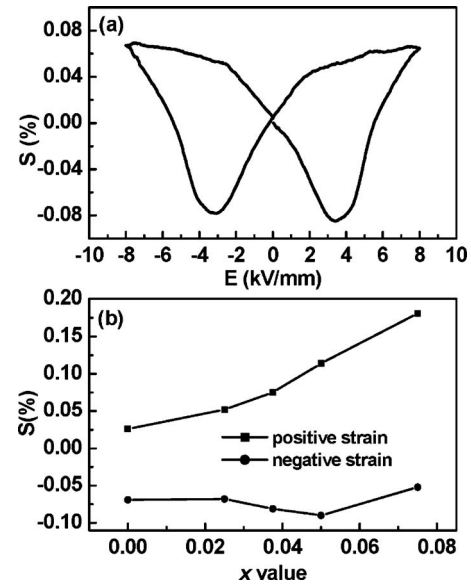


FIG. 5. (a) Bipolar S-E curve of the composition with $x=0.0375$ and (b) composition dependent maximum positive strain and negative strain.

P_s and P_r increase slightly before $x \leq 0.0375$, reaches the maximum at $x=0.0375$ with $P_s=42.0 \mu\text{C}/\text{cm}^2$ and $P_r=36.5 \mu\text{C}/\text{cm}^2$, then tend to decrease dramatically with further increasing x . Especially, one can see that the difference between P_s and P_r keeps almost constant when $x \leq 0.0375$ and then becomes large when $x=0.050$ and 0.075 , indicating that the loops tend to be slim. On the other hand, E_c decreases monotonously with increasing x , with a sudden decrease from $4.6 \text{ kV}/\text{mm}$ for the composition with $x=0.025$ to $3.5 \text{ kV}/\text{mm}$ for the composition with $x=0.0375$, which maybe attributed to the fact that the MPB structure is located near $x=0.0375$.

Bipolar S-E curve of the composition with $x=0.0375$ is shown in Fig. 5(a). Generally, all compositions exhibit a typical butterfly shaped bipolar S-E curves, indicating the ferroelectric nature of the ceramics, consistent with the above P-E loops. To further clarify the composition dependence of S-E shape in detail, we plot the maximum positive strain and negative strain against x value, as shown in Fig. 5(b). Both the positive and negative strain values increases with increasing x , except a decreasing negative strain value from $x=0.050$ to $x=0.075$. The increased strain value may be related to the decreased T_d , which is the ferroelectric-antiferroelectric transition temperature in BNT-based materials, of this system, as indicated in Fig. 3(b). Larger x value, lower T_d , that means the composition with $x=0.075$ is most close to T_d , therefore, this composition is most close to antiferroelectric order at room temperature. At room temperature, the composition closer to T_d will have larger strain because under an applied electric field, antiferroelectric can transit into ferroelectric state, this field-assisted phase transition generally is accompanied by large strain.⁹ Actually, similar results are observed and discussed in other BNT-based piezoceramics systems.^{7,15}

Unipolar S-E curves are also measured and displayed, the typical unipolar S-E curve of the composition with $x=0.0375$ is shown in Fig. 6. The inset indicates the compo-

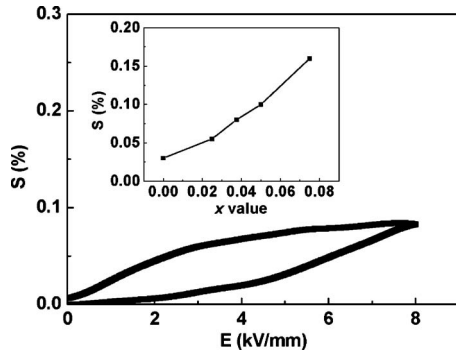


FIG. 6. Unipolar S-E curve of the composition with $x=0.0375$, the inset plots the composition dependent unipolar strain value.

sition dependent unipolar strain value, which increases monotonously with increasing x , consistent with the above composition dependence of bipolar strain and with the composition dependence of bipolar/unipolar strain of other reported BNT-based lead-free piezoceramics with well saturated P-E loops,⁷ but lower than that with slim P-E loops.¹⁵

Figure 7 shows the piezoelectric coefficient (d_{33}) and planar coupling factor (k_p) as the functions of x . It is worth noting that the piezoelectric properties are comparable with other BNT-based lead-free piezoceramics.^{2,6,7,15} Highest d_{33} and k_p values of 92 pC/N and 0.22, respectively, are obtained in the MPB composition with $x=0.0375$. No obvious resonant and antiresonant peaks can be detected in the poled ceramics with $x=0.075$, so we cannot obtain its k_p value.

IV. CONCLUSION

In summary, single phase $(1-x)\text{BNT}-x\text{BZT}$ lead-free piezoceramics were prepared and the structures and properties were investigated. The introduction of BZT leads to increased Curie temperature of BNT. A rhombohedral-tetragonal MPB is located near $x=0.0375$. As a result, this MPB composition shows improved ferroelectric and piezoelectric properties. The composition dependence of both bipolar strain and unipolar strain is discussed by considering effects of BZT on depolarization temperature. Our results are an interesting supplement for BNT-based lead-free piezoceramics and may provide some guideline to the search for new lead-free piezoceramics with high Curie temperature.

ACKNOWLEDGMENTS

The authors acknowledge the helpful discussions from Dr. A. Kouna. This work was jointly supported by the Hong

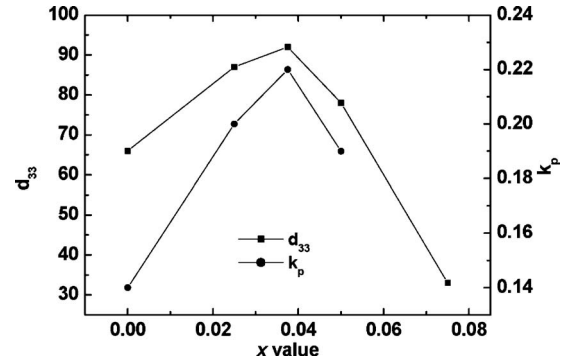


FIG. 7. Piezoelectric coefficient and coupling factor as the functions of composition.

Kong Polytechnic University (A-PH92), the research foundation for returned overseas Chinese scholar, National Nature Science Foundation of China (Grant Nos. 10874069 and 10704021), the new century excellent talents in university (NCET-08-0279), and Natural Scientific Research Innovation Foundation in Harbin Institute of Technology (Grant No. HIT.NSRIF 201055).

- ¹J. Rödel, W. Jo, K. T. P. Seifert, E.-M. Anton, and T. Granzow, *J. Am. Ceram. Soc.* **92**, 1153 (2009).
- ²S. J. Zhang, R. Xia, and T. R. Shrout, *J. Electroceram.* **19**, 251 (2007).
- ³Y. Saito, H. Takao, T. Tani, T. Nonoyama, K. Takator, T. Homma, T. Nagaya, and M. Nakamura, *Nature (London)* **432**, 84 (2004).
- ⁴E. Hollenstein, M. Davis, D. Damjanovic, and N. Setter, *Appl. Phys. Lett.* **87**, 182905 (2005).
- ⁵Y. Guo, K. Kakimoto, and H. Ohsato, *Jpn. J. Appl. Phys., Part 1* **43**, 6662 (2004).
- ⁶T. Takenaka, K. Maruyama, and K. Sakata, *Jpn. J. Appl. Phys., Part 1* **30**, 2236 (1991).
- ⁷A. B. Kouna, S. T. Zhang, W. Jo, T. Granzow, and J. Rödel, *Appl. Phys. Lett.* **92**, 222902 (2008).
- ⁸H. Yu and Z.-G. Ye, *Appl. Phys. Lett.* **93**, 112902 (2008).
- ⁹S. T. Zhang, A. B. Kouna, E. Aulbach, H. Ehrenberg, and J. Rödel, *Appl. Phys. Lett.* **91**, 112906 (2007).
- ¹⁰M. R. Suchomel, A. M. Fogg, M. Allix, H. Niu, J. B. Claridge, and M. J. Rosseinsky, *Chem. Mater.* **18**, 4987 (2006).
- ¹¹M. R. Suchomel and P. K. Davies, *Appl. Phys. Lett.* **86**, 262905 (2005).
- ¹²I. Grinberg, M. R. Suchomel, W. Dmowski, S. E. Mason, H. Wu, P. K. Davies, and A. M. Rappe, *Phys. Rev. Lett.* **98**, 107601 (2007).
- ¹³J. Chen, P. H. Hu, X. Y. Sun, C. Sun, and X. R. Xing, *Appl. Phys. Lett.* **91**, 171907 (2007).
- ¹⁴X. D. Zhang, D. Kwon, and B. G. Kim, *Appl. Phys. Lett.* **92**, 082906 (2008).
- ¹⁵Y. Hiruma, H. Nagata, and T. Takenaka, *Appl. Phys. Lett.* **95**, 052903 (2009).